ORIGINAL ARTICLE

Gap junctions regulate vessel diameter in chick chorioallantoic membrane vasculature by both tone-dependent and structural mechanisms

Martin Maibier[1,2] | Willem Bintig[1,3] | Andrean Goede[1,2] | Michael Höpfner[1,2] |
Wolfgang M. Kuebler[1,2,4,5,6] | Timothy W. Secomb[7] | Bianca Nitzsche[1,4] iD |
Axel R. Pries[1,8]

[1]Charité - Universitätsmedizin
Berlin, Corporate Member of Freie
Universität Berlin, Humboldt - Universität zu
Berlin, Berlin, Germany

[2]Institute of Physiology, Berlin Institute of
Health, Berlin, Germany

[3]Institute of Biochemistry & Neuro Cure
Cluster of Excellence, Berlin Institute of
Health, Charité - Universitätsmedizin Berlin,
Berlin, Germany

[4]DZHK (German Centre for Cardiovascular
Research), partner site Berlin, Berlin,
Germany

[5]Keenan Research Centre for Biomedical
Science, St. Michael's Hospital, Toronto, ON,
Canada

[6]Departments of Surgery and
Physiology, University of Toronto, Toronto,
ON, Canada

[7]Department of Physiology, University of
Arizona, Tucson, Arizona

[8]German Heart Center Berlin, Berlin,
Germany

Correspondence
Bianca Nitzsche, Charité –
Universitätsmedizin Berlin, Charitéplatz 1,
10117 Berlin, Germany.
Email: bianca.nitzsche@charite.de

Abstract

Objective: In this study, we examined the impact of gap junction blockade on chick chorioallantoic membrane microvessels.

Methods: Expression of Cx37, Cx40/42, and Cx43 in chick chorioallantoic membrane tissue was studied by PCR, Western blot, and confocal immunofluorescence microscopy. Vessel diameter changes occurring under gap junction blockade with carbenoxolone (175 µmol/L), palmitoleic acid (100 µmol/L), [43]GAP27 (1 mmol/L) were analyzed by intravital microscopy. To analyze vascular tone, chick chorioallantoic membrane vessels were exposed to a vasodilator cocktail consisting of acetylcholine (10 µmol/L), adenosine (100 µmol/L), papaverine (200 µmol/L), and sodium nitroprusside (10 µmol/L).

Results: In chick chorioallantoic membrane lysates, Western blot analysis revealed the expression of Cx40 and Cx43. Immunofluorescence in intact chick chorioallantoic membrane vasculature showed only Cx43, limited to arterial vessel walls. Upon gap junction blockade (3 hours) arterial and venous diameters decreased to 0.50 ± 0.03 and 0.36 ± 0.06 (carbenoxolone), 0.72 ± 0.08 and 0.63 ± 0.15 (palmitoleic acid) and 0.77 ± 0.004 and 0.58 ± 0.05 (GAP27), relative to initial values. Initially, diameter decrease was dominated by increasing vascular tone. After 6 hours, however, vessel tone was reduced, suggesting structural network remodeling.

Conclusions: Our findings suggest a major role for connexins in mediating acute and chronic diameter changes in developing vascular networks.

- -

1 | INTRODUCTION

Gap junctions mediate intercellular communication. Composed of two hexamer transmembrane spanning hemichannels, called connexons, they allow the exchange of small molecules (<1 kDa) and ions by bridging the extracellular space of neighboring cells thereby connecting their cytoplasm.[1] Each connexon consists of six Cx. Among the more than 20 Cx isoforms Cx37 (GJA4), Cx40 (GJA5), and Cx43 (GJA1) are the ones predominantly expressed in blood vessels.[2-4]

Several studies have shown the importance of Cxs for vascular function and development. Knockout mice lacking GJA4 and GJA5 show severe vascular dysmorphogenesis with distended blood vessels and hemorrhages.[5,6] In vitro, siRNA knockdown of GJA4, GJA5, or GJA1 in human umbilical vein endothelial cells resulted in decreased branch formation in tube formation assays.[7] The group of Duling showed that knockout of endothelial Cx43 resulted in hypotension, bradycardia, and elevated plasma levels of NO and angiotensin I and II in mice.[8] Furthermore, GJ-based communication is considered essential for the propagation of vasomotor responses along arterial vessels.[9-11]

However, our current understanding of vascular GJs and their function in vascular maintenance and adaptation is mainly based on in vitro studies which can not address the interdependency and interactions of coupled blood vessels in microvascular networks of the living organism. Pioneering in vivo experiments analyzing the role of GJs in the murine microcirculation were carried out by the groups of Segal and DeWit.[9,12-16] Both authors showed the importance of Cxs in mediating vasomotor responses and dissected the different conduction pathways involved. Still, even these groundbreaking experiments were limited to the analysis of single blood vessels and only suitable for investigating acute (but not prolonged) vessel changes. Consequently, the role of GJs for homeostasis and adaptation of functional microvascular networks remains unclear.

In previous work, we proposed a possible role for GJs-based communication in structural adaptation of vascular beds. Based on mathematical models for adaptation of vessel diameters, we predicted that microvascular networks regulated by local hemodynamic (pressure, shear stress) and metabolic stimuli cannot generate functionally adequate flow distributions unless information transfer along the wall of blood vessels (conducted response) also acts as a stimulus for structural adaptation.[17-19] Conversely, absence of conducted stimuli is expected to lead to functional shunting and malperfusion.[20,21]

To test this hypothesis, we investigated the role of vascular Cxs in the regulation of vessel diameters in functional vascular networks of the CAM model of fertilized chicken eggs. Since conducted responses may contribute to both acute (tone-dependent) and structural regulation of diameters, we also observed vessel diameters when exposed to a vasodilator cocktail. Changes in diameters of fully dilated vessels were considered to represent structural remodeling.

2 | MATERIALS AND METHODS

2.1 | Ex ovo CAM model

The ex ovo CAM model was used as previously described.[22] Briefly, fertilized white leghorn chicken eggs (Gallus gallus, VALO BioMedia GmbH) were incubated in horizontal position at a temperature of 37.5°C and relative humidity of 60%-80%. After 72 hours, the eggshell was cracked under aseptic conditions; the embryonated eggs were placed in plastic culture dishes (TPP, internal diameter: 88 mm) and kept in a humidified environment at 37.5°C until chick embryos reached HH stage 40-42, which corresponds to day 14 of embryonic development.

2.2 | Intravital microscopy

For intravital microscopy, culture dishes were placed on a custom-made, temperature and humidity-controlled microscopic stage. The microscope (Axiotech) was equipped with two objectives (2.5×, NA 0.085; 5×, NA 0.16; Zeiss, transillumination) and CAM vascular networks were visualized for up to 24 hours. Microscopic images were taken using a CCD camera (CX9000, MBF Bioscience) and processed by appropriate image analysis software (Neurolucida, Vs8; MBF Bioscience). Video sequences were recorded using a CMOS camera (Sony ICE600). Vessel diameters were measured using ImageJ Vs 1.51n software.[23,24] After treatment with Cx blockers, a fraction of blood vessels could not be visualized anymore due to diameter reduction and impaired blood flow (see Figure 2A). Their post-treatment diameter was arbitrarily set to 5 μm.

2.3 | Reverse transcription polymerase chain reaction

Total RNA was extracted from CAM samples at development day 14 and purified using RNeasy Mini Kit following the manufacturer's instructions (Qiagen). Samples were treated with ribonuclease-free deoxyribonuclease (DNASEI; Qiagen) to remove any genomic DNA contamination. RNA concentration and purity were measured spectrophotometrically at wavelengths of 260 and 280 nm, respectively. cDNA was synthesized by RT of 2 μg of total RNA using the Phusion RT-PCR Kit (Thermo Fisher Scientific) according to the manufacturer's protocol. Reverse transcription PCR was carried out in a total volume

TABLE 1 RT-PCR primers used for the detection of endothelial Cxs in chicken CAM tissue

Name	Primer (5'-3')	Gene bank accession number	Product size (bp)	Denaturing temperature and time (s)	Annealing temperature and time (s)	Extension temperature and time (s)	Number of cycles	Sequence identity to human mRNA (%)
Cx37 (GJA4)	F:CTC TGC TCT CTG CTG TTT TCC C R:TCC TAC ACT GAT GCC AAG TCC C	NM_206984.3	117	94°C (60)	65°C (45)	72°C (120)	35	79
Cx40/42 (GJA5)	F:GCA AAC ACT TCA GTC AGC CAC C R:GAA CAG CAC AGT CAA CCA GAC C	NM_205504.2	203	94°C (15)	65°C (45)	72°C (60)	35	73
Cx43 (GJA1)	F:TGA CAA GTC CTT CCC CAT CTC C R:CAG TCC TCC ACG CAT CTT TAC C	NM_204586.2	256	94°C (60)	65°C (45)	72°C (120)	35	79
ß-Actin	F:CCC CAA AGC CAA CAG AGA GAA G R:ATG AGG TAG TCC GTC AGG TCA C	NM_205518.1	237	94°C (15)	65°C (45)	72°C (60)	35	84

of 50 μL containing 250 nmol/L of each primer, 500 μmol/L deoxyribonucleotide triphosphate, 25 mmol/L $MgCl_2$, and 1 U Phusion Hot Start II DNA-Polymerase. Primer pairs were combined and diluted to a final concentration of 10 μmol/L. Primer sequences, annealing/extension temperatures, and gene bank accession numbers are listed in Table 1. RT-PCR was performed in a Peltier thermal cycler (PTC-200; MJ-Research).

2.4 | Western blotting

Western blotting was performed as described.[25] CAM tissue lysates were prepared by excision of 5 mm^2 of CAM tissue, which was washed two times with ice-cold PBS, lysed in ice-cold RIPA buffer supplemented with protease inhibitors (Roche cOmplete, Mini Protease Inhibitor Cocktail) and subsequently homogenized with a homogenizer (Minilys, Bertin Instruments). Homogenates were centrifuged at 20 000 *g*, and supernatant was collected for protein quantification analysis using BCA Thermo Scientific Pierce™ Protein Assay. Fifteen-twenty microgram of protein was loaded on an SDS-PAGE gel. Proteins were transferred to nitrocellulose membrane using a wet blot tank system (Bio-Rad) for 2 hours. Membranes were blocked for 1 hour at room temperature with 5% skim milk in TBS-T before incubation with primary (overnight, 4°C) and secondary (1 hour, room temperature) antibodies in TBS-T. In between and after incubation, membranes were washed three times with TBS-T at room temperature for 10 minutes. Antibody-stained proteins were visualized using the Fusion SL system from Vilber and ECL Select Western Blotting Detection Reagent (GE Healthcare).

2.5 | Antibodies

Given the high conservation of amino acid sequences of Cx isoforms in different species, we were able to use commercially available, rabbit polyclonal, primary antibodies directed against murine (Cx37), or human Cxs (Cx40, Cx43) to test for the expression of chick Cxs.[3,26] GJA5 encodes for Cx42 in chicken and Cx40 in mammals and we used two different Cx40 antibodies to analyze its expression patterns. Table 2 shows the primary antibodies used for immunoblotting and immunofluorescence and sequence identity between their respective binding regions in mice/humans and chick (as given by Basic Local Alignment Search Tool [BLAST] analysis, available at https://www.ncbi.nlm.nih.gov). Selectivity and specificity of the used antibodies were investigated by checking whether Western blots revealed a single protein band at the expected molecular weight (Figure 1). Negative controls were performed by omitting the primary antibody. For immunoblotting, secondary, peroxidase-labeled antibodies (Vector Laboratories, PI-1000 and PI-2000) were used at 1:3000-1:10 000. For immunofluorescence, primary antibodies against desmin (Dako, M0760292) were used at 1:33. Secondary fluorescence-labeled antibodies (goat anti-mouse 568, A11031 and goat anti-rabbit 488; Invitrogen) were diluted in a ratio of 1:200.

TABLE 2 Primary antibodies used for immunoblotting and immunofluorescence

| Name	Antibody name (company)	Antibody-binding site	Sequence identity between antibody-binding site and respective amino acid sequence in chick	Dilution for immunoblotting (immunofluorescence)
Cx37 (Gja4)	Ab58918 (Abcam)	N-terminal amino acids 73-122 of murine Cx37	80% (40/50)	1:2000
Cx40/42 (Gja5)	SAB1304973 (Sigma)	N-terminal region of human Cx40	89% (158/177)[a]	1:1000 (1:200)
	Ab183648 (Abcam)	Internal sequence of human Cx40	[b]	1:2000
Cx43 (Gja1)	C6219 (Sigma)	C-terminal amino acids 363-382 of human Cx43	95% (19/20)	1:5000-1:10 000 (1:100)

[a]The SAB1304973 antibody targets the N-terminal sequence of human Cx40. Here, sequence identity between chick and human is 89% (158/177).
[b]The binding site was of the Ab183648 antibody was not specified. According to the manufacturer, species reactivity includes chick Cx 42.

2.6 | Confocal immunofluorescence microscopy

For imaging and staining of vascular membranes, 5 mm² of CAM tissue was excised from the fertilized chicken egg at HH 40-42. CAM tissue was washed twice with PBS (pH 7.4), then fixed with 4% PFA, 4% sucrose in PBS for 20-40 minutes, permeabilized with 0.2% TritonX-100/PBS solution for 30 minutes and blocked with blocking solution (1% goat serum, 2% BSA, 0.1% sodium acid, 0.2% TritonX-100)

for 1 hour. Primary and secondary antibodies were diluted in blocking solution and incubated overnight at 4°C. In between and after the incubation with antibodies, CAM tissue was washed three times with PBS for 10-30 minutes. CAM tissue was covered with ProLong Gold antifade reagent (Invitrogen), and images were acquired using a Leica SP5 inverse laser confocal microscope (Microsystems GmbH) equipped with 20/40/63x objectives. The fluorescence channels were separately acquired by a sequential scanning mode.
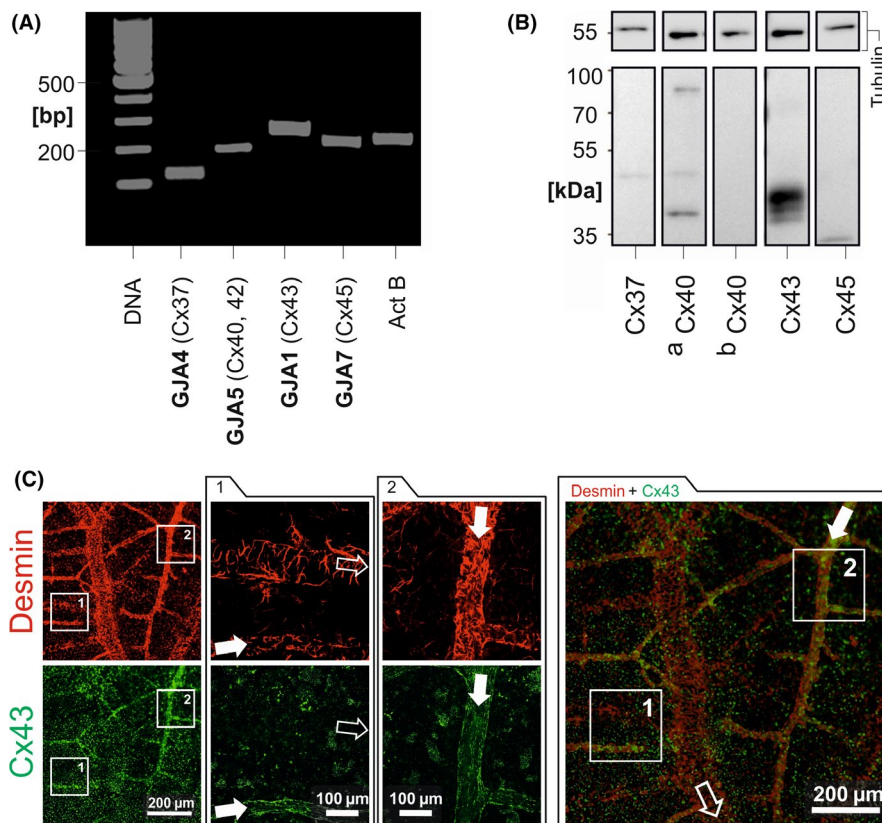
FIGURE 1 Expression and localization of Cxs in the CAM. A, Qualitative RT-PCR revealed mRNA expression of GJA4 (Cx37), GJA5 (encoding for Cx40 in mammals and Cx42 in chicken), and GJA1 (Cx43) in CAM tissue. beta-Actin (ActB) served as loading control. B, Immunoblotting confirmed protein expression of Cx40/42 and Cx43. Cx37 was not found in CAM lysates. To test for Cx40/42 expression, two different antibodies were used (see section 2 and Table 2). The antibody targeting the N-terminal region of human Cx40 (a) consistently detected Cx40/42, whereas the one designed against an internal sequence of human Cx40 (b) did not. C, Representative immunofluorescence pictures of CAM vascular networks. Staining with the pericyte/smooth muscle cell marker desmin allowed tracking of arterial and venous vessels (upper panel). Staining for Cx43 revealed localization in ART (filled arrows) at the membrane of neighboring cells (detail 1, 2, and merged image). In VEN (open arrows), the signal was not specific (detail 1 and merged image). Cx40/42 was not detected by CFM. CAMs of n = 3 chick embryos were used for all experiments
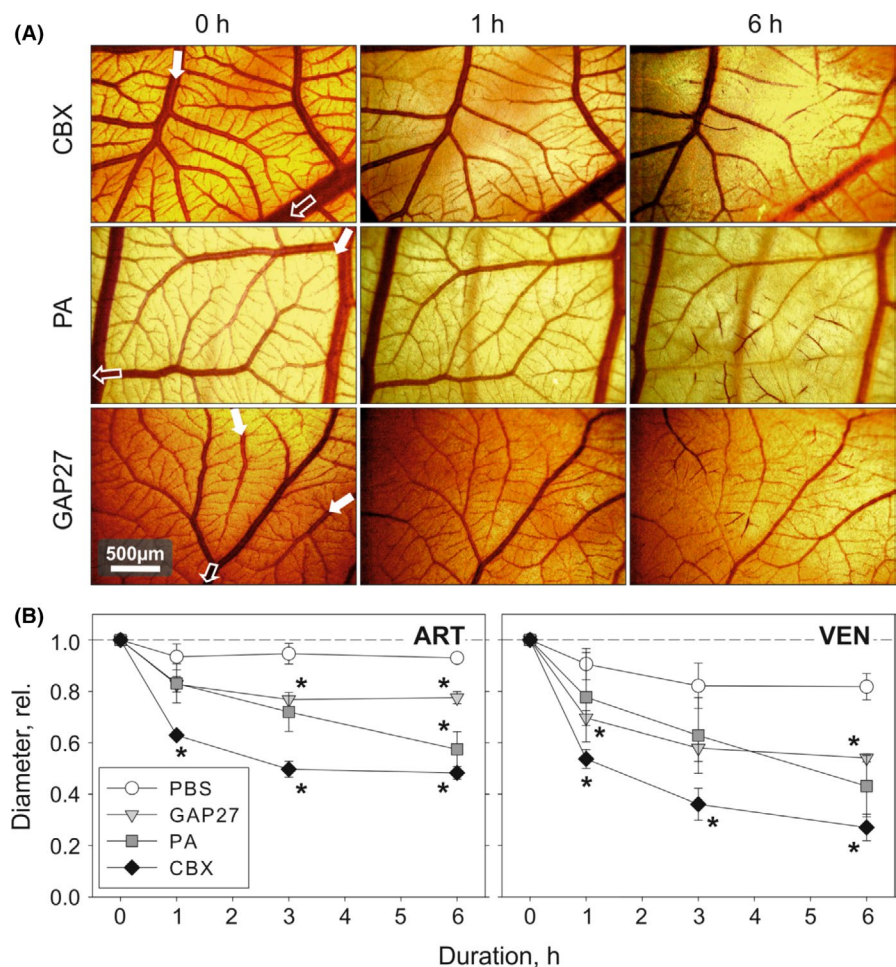
2.7 | Cell culture

The permanent somatic endothelial cell line EA.hy926 (ATCC CRL-2922) was maintained in DMEM (Biochrom AG) with 10% fetal bovine serum, 100 U/mL penicillin, and 100 mg/mL streptomycin and cultured at 37°C in a humidified atmosphere of 5% CO_2. Cell culture medium was changed every second day, and once a week, the cells were passaged using 1% Trypsin/EDTA.

2.8 | Determination of cytotoxicity

EA.hy926 cells were seeded at a density of 4000 cells/well into 96-well microtiter plates and incubated with the unspecific GJs blockers CBX (50, 175, 400 µmol/L) and PA (100 µmol/L) for 1-6 hours. One hundred microliter of each sample was incubated with 100 µL LDH assay reagent for 10 minutes at room temperature in the dark. Release of LDH was determined by a colorimetric kit as described previously.[27] Extinction (E) was measured at 490 nm. Cytotoxicity of a specific compound was calculated as

$$\text{Cytotoxicity}\,(\%) = \frac{E_{\text{compound}} - E_{\text{low control}}}{E_{\text{high control}} - E_{\text{low control}}} \times 100$$

where $E_{\text{low control}}$ is the extinction of PBS-treated cells that were used as negative control. $E_{\text{high control}}$ is the extinction after treatment with 100 µL 2% (v/v) Triton X-100 which served as positive control.

2.9 | Pharmacological modulation of gap junction function

Effects of the following GJ blockers (all purchased from Sigma Aldrich) on arterial and venous vessel diameters were determined:

- Carbenoxolone—the glycyrrhizin acid metabolite CBX is a non-specific inhibitor of intercellular communication commonly applied in concentrations of about 100 µmol/L.[28-30] Here, we used increasing concentrations from 25 to 400 µmol/L.
- Palmitoleic acid—the fatty acid PA, which disrupts GJ communication by intercalation in the lipid bilayer, blocks Cx40 and Cx43 in working concentrations up to 50 µmol/L.[31-33] Since PA is poorly water-soluble and easily oxidized, working solutions (100 µmol/L) were prepared under nitrogen atmosphere out of PA stock solutions (100 mmol/L) in DMSO. The concentration of DMSO in working solutions was 0.1%.
- GAP27—the GJ blocking peptide GAP27 mimics amino acids 204-214 (SRPTEKTIFII) on the extracellular loop 2 of Cx43 blocking GJ communication by disturbing connexon assembly.[26] The SRPTEKTIFII

FIGURE 2 Treatment with the non-specific GJ blockers CBX (175 µmol/L) and PA (100 µmol/L) as well as the specific GJ blocker GAP27 (1000 µmol/L) reduced diameter of arterial and venous vessels in the CAM. A, Intravital micrographs of CAM sections before, after 1 and 6 h of treatment. Arterial vessels and flow directions are indicated by filled arrows, VEN and venous flow directions by open arrows. B, Time-dependent changes in relative arterial and venous vessel diameter. For CBX and GAP27, about 60% (90%) of the diameter decrease occurred after 1 h (3 h) of treatment. Diameter decline upon PA treatment was more linear with about one-third of diameter reduction occurring at 1, 3, and 6 h, respectively. Due to shrinking and impaired blood flow, some blood vessels could not be visualized after Cx blockade. For each substance, at least N = 122 ART (VEN) were analyzed in n = 3 CAMs. For ART (VEN), initial diameters ranged from 11 to 247 µm (11-193 µm). Data are given as means ± SEM, * $P < .05$ vs PBS control was considered statistically significant

sequence is completely conserved in chick Cx43, except that isoleucine (position 214 in human Cx43) is replaced by valine, which is also a non-polar amino acid like isoleucine. GAP27 concentration used for experiments was 1000 µmol/L. Combination of GJ blocking peptides may increase their efficacy.[34] Here, however, only one peptide was used.

All GJ blockers were dissolved in PBS and applied every 2 hours ($t = 0$, 2, 4 hours) in drops of 25 µL to warrant a permanent coverage of the investigated CAM areas.

Additionally, we studied the effects of the GJ function stimulating agent DIP. DIP increases the concentration of cytosolic cAMP which is believed to increase GJ coupling via different pathways such as elevated Cx trafficking, changes in phosphorylation status and increased Cx expression.[35] Chick chorioallantoic membrane vasculature was exposed for 24 hours to PBS (control), 175 µmol/L CBX, 50 µmol/L DIP, or a combination of CBX and DIP for 24 hours. For these experiments, 20 µL of 175 µmol/L CBX was applied topically at the beginning of the experiment. DIP was dissolved in DMSO (10 mmol/L) and diluted in PBS at 1:200.

2.10 | Vascular tone of CAM vessels

In order to determine VT of arteriolar and venous CAM vessels, 75 µL of a vasodilator cocktail consisting of 10 µmol/L Ach (Sigma Aldrich), 100 µmol/L ADO (Serva Feinbiochemica), 200 µmol/L PAP (Sigma Aldrich), and 10 µmol/L SNP (Sigma) dissolved in PBS was applied on either native (for determination of resting tone) or CBX-treated CAM vessels for 15 minutes to achieve maximal vessel dilatation. Vascular tone was expressed as

$$VT = \frac{D_{max} - D}{D_{max}}$$

where D_{max} is the maximal diameter after application of the dilatory cocktail and D is the vessel diameter before dilatation (resting diameter or diameter after CBX treatment, respectively).

2.11 | Statistical analysis

For RT-PCR, Western Blotting and immunofluorescence, at least n = 3 CAMs per experiment were used. For each substance and/ or concentration applied on CAM vessels, a minimum of N = 20 ART and 20 VEN were analyzed. If not stated otherwise, each CAM experiment was independently reproduced three times (n = 3 CAMs). Data are given as mean ± SEM. Diameter changes were analyzed using Student's *t* test; a *P*-value < .05 was considered significant.

3 | RESULTS

3.1 | Connexin 43 is abundantly expressed in arterial CAM vessels

In order to screen for Cxs potentially expressed in CAM tissue, we performed RT-PCR which revealed mRNA expression of Cx37 (GJA1), Cx40/42 (GJA5), and Cx43 (GJA4; Figure 1A).


FIGURE 3 CAM ART (top) and VEN (bottom) incubated for 3 h with different CBX concentrations showed dose-dependent diameter decrease and stasis of blood flow. Significant vessel diameter reduction was limited to higher CBX concentrations starting at 100 µmol/L. Concentrations of 175 µmol/L and above also caused blood flow stasis in both ART and VEN. For each concentration, a minimum of each N = 90 ART and VEN were analyzed in n = 3 networks (except for CBX 100 µmol/L, n = 2). Asterisk indicates statistically significant diameter difference vs control substance PBS, P < .05

Western blotting for protein expression of the respective mRNA revealed the presence of Cx40/42 and Cx43 (Figure 1B). Among the two antibodies used to analyze Cx40/42 expression (Table 2), only the SAB1304973 antibody targeting the N-terminal region of Cx40/42 consistently detected Cx40/42 so that it was used for further experiments.

To determine spatial distribution of Cx40/42 and Cx43 in CAM tissues, CFM was carried out and only Cx43 was detected. Cx43 was ubiquitously expressed in arterial (Figure 1C, detail 2, lower panel) but not venous vessel walls (Figure 1C, detail 1, lower panel). Staining with the pericyte/ smooth muscle cell marker desmin allowed tracking of arterial and venous vessels (Figure 1C, upper panel).

3.2 | Connexin blockers cause arterial and venous vessel diameter decrease

To test whether the observed protein expression had functional relevance in intact CAM vasculature, we treated CAM networks with the non-specific Cx blockers CBX and PA as well as the Cx43 specific blocker GAP27 (Figure 2A). All inhibitors decreased vessel diameters in both ART and VEN (Figure 2B).
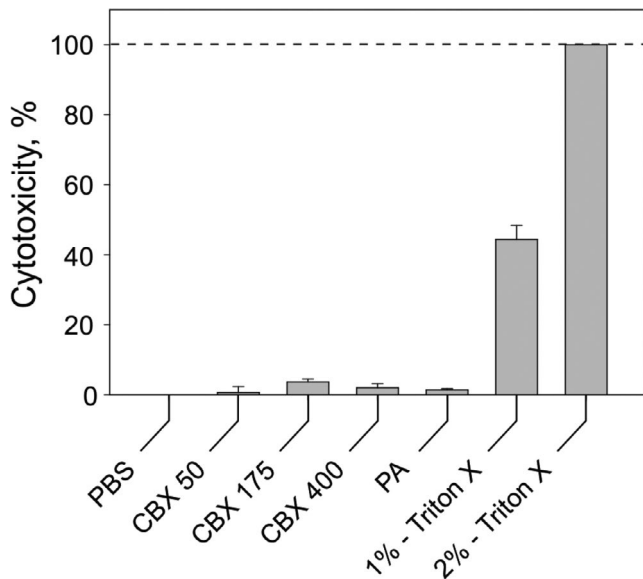
FIGURE 4 The non-specific GJ blockers CBX and PA had no relevant cytotoxic effects on EA.hy926 endothelial cells. Cytotoxicity was calculated by measuring the amount of LDH release after treatment with CBX (50, 175, 400 µmol/L) and PA (100 µmol/L) for 6 h. PBS-treated cells were used as negative controls. Cells treated with 2%—TritonX100 served as positive controls. Data are given as means ± SEM, n = 3

For further experiments, we focused on CBX as the effects on vessel diameter were most pronounced for this substance. CBX is a small and stable molecule. PA, however, can lose its function through oxygenation and the molecular weight of GAP27 is roughly twice as big as the one of CBX, potentially causing poorer accessibility to CAM vessels. Also, CBX blocks all Cxs potentially involved, including Cx40/42 which might play a role in mediating GJ intercellular communication in CAM vessels despite it could be only detected by Western blotting and not by CFM in the present study.

CBX showed dose-dependent effects on CAM vessels (Figure 3). Concentrations of more than 25 µmol/L led to significant diameter decrease in both arterial and venous vessels. Concentrations of 175 µmol/L or higher additionally caused concomitant stasis of blood flow in both vessel types.

3.3 | Connexin blockers do not cause unspecific effects

We wanted to exclude the possibility that the effects occurring under the application of CBX and PA are non-specific. Firstly, we carried out LDH assays to test for eventual cytotoxicity of the non-specific Cx blockers CBX and PA. As shown in Figure 4, neither CBX nor PA had relevant cytotoxic effects on EA.hy926 endothelial cells. Secondly, we investigated whether DIP, which stimulates Cx function, limits the effects of CBX on CAM vasculature. Figure 5A shows intravital micrographs of CAM sections treated with PBS (control), CBX, DIP, or a combination of CBX and DIP. In accordance with the data given in Figure 2, vessel diameters decreased significantly upon CBX treatment (Figure 5B). In the presence of DIP, however,

CBX-induced vessel diameter reduction was abolished suggesting that the observed effects are mediated by changes in Cx function rather than being non-specific.

3.4 | CBX-induced vessel diameter decrease is mediated by tone-dependent and tone-independent mechanisms

In order to evaluate the role of VT before and during Cx blockade, we applied a vasodilator cocktail consisting of Ach, ADO, PAP, and SNP on untreated and CBX-treated CAM networks (Figure 6).

Vascular tone of arterial (10 ± 1%) and venous vessels (6 ± 4%) was low under resting conditions. Initially, increase of VT contributed significantly to the CBX-induced vessel diameter reduction: more than half of the diameter decrease of ART and VEN that occurred within the first 3 hours after CBX treatment could be reversed by maximal vasodilatation. After 6 hours of CBX treatment, however, vasodilatory responses were strongly reduced, indicating that diameter reduction had become structurally fixed.

4 | DISCUSSION

It has been extensively shown that vascular GJs provide the basis for the propagation of local vasodilatory and vasoconstrictive stimuli by allowing the passage of ions and small molecules between adjacent cells of the vessel wall.[13,36,37] However, most of our knowledge on vascular GJ function is deduced from in vitro studies or investigations of single blood vessels, ignoring the interdependency of coupled blood vessels in microvascular networks. Also, a little is known about the importance of GJs for mediating prolonged vascular changes, as most of the studies have investigated their role as mediators of acute vasomotor responses.

In this study, we examined the role of Cxs for the acute and prolonged regulation of vessel diameter in functional networks of the CAM vasculature, the avian homologue of human fetoplacental circulation. This in vivo model allows live observation for extended durations of up to 24 hours and thus tracking of sustained and structural changes.

We found that Cx43 is ubiquitously expressed in arterial but not venous CAM vessel walls (Figure 1C) and that Cx blockade with the non-specific inhibitors CBX, PA as well as the specific inhibitor GAP27 led to diameter decrease in both arterial and venous vessels (Figure 2). This effect is likely to be specific to Cx blockade since none of the unspecific blockers showed relevant cytotoxicity on EA.hy926 endothelial cells (Figure 4), and vessel diameter reduction under CBX treatment was abolished in the presence of the GJ stimulating agent DIP (Figure 5). The contribution of increased VT was relevant for the early phase up to about 3 hours but decreased strongly after 6 hours, suggesting an increasing structural fixation of diameter decrease (Figure 6).

The local expression pattern of vascular Cxs differs between different blood vessel types, different cells of the vascular wall, and
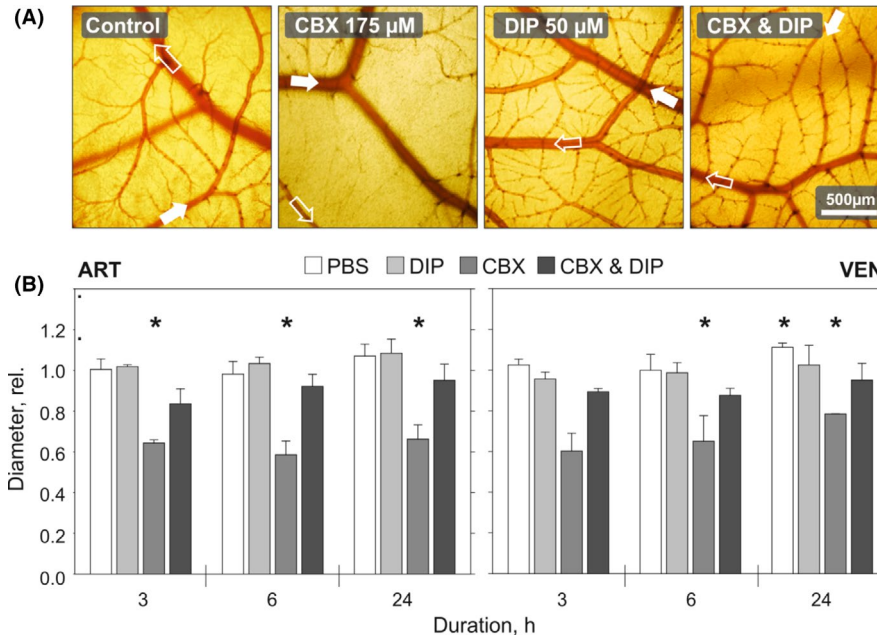
FIGURE 5 Co-incubation with DIP abolished CBX-induced vessel diameter decrease. A, Intravital micrographs of CAM sections treated for 24 h with PBS (control), CBX (175 μmol/L), DIP (50 μmol/L), and a combination of both. Arterial (venous) flow direction is indicated by filled (open) arrows. B, Quantification of relative arterial and venous vessel diameter after 3, 6, and 24 h of incubation. CBX-induced vessel diameter reduction was not observed in the presence of DIP. For both, PBS-treated ART (1 → 1.07, P = .13) and VEN (1 → 1.11, P < .05), relative vessel diameter increases over 24 h reflecting vascular growth. In this set of experiments, diameter of venous vessels treated for 3 h with CBX was not significantly reduced (1 → 0.6, P = .14, N = 2). However, these data point toward the results given in Figures 2 and 3 where a significant diameter difference is reported for VEN treated with CBX for 3 h. A minimum of each N = 20 ART and VEN were analyzed in n = 2-4 CAM networks. Data are shown as means ± SEM, * P < .05 vs PBS control t_0

different species.[38] To our knowledge, Cx expression has not been investigated in CAM vasculature so far and it is surprising that Cx43, and not Cx40/42, seems primarily responsible for mediating conducted responses in CAM vessels.

From the known functions of Cxs and the present observations in the CAM, the following hypotheses may be derived:

- Gap junctions are abundantly expressed on the arterial side of CAM vasculature to ensure propagation of vasodilatory stimuli, putatively generated at the capillary level.
- These stimuli are needed to keep VT of upstream arterial vessels at a low level and thus prevent acute arterial flow reduction and long-term regression or even collapse of these vessels.
- Since arterial and venous vessels are hemodynamically coupled, arterial diameter decrease also causes reduced pressure, volume flow, and shear stress in venous vessels resulting in attenuated release of vasodilatory substances, that is, NO,[39,40] and increased VT and structural diameter decrease.

If vessel diameter reduction exceeds a certain threshold, blood flow is impaired. For CBX concentrations of 175 μmol/L or higher, blood flow stasis was observed in both arterial and venous vessels (Figure 3). Since flow resistance is inversely dependent on the fourth power of vessel diameter (Poiseuille's law), vessel diameter reduction of approximately 50% as seen under treatment with 175 μmol/L CBX causes a 16-fold increase of blood flow resistance which leads to

malperfusion and eventually blood flow stasis in the supplied area of the CAM.

Previous studies have investigated the relationship between blood flow velocity, mechanical stress, and Cx43 expression. It has been reported, that Cx43 mRNA increased in endothelial cells subjected to sustained levels of mechanical strain and fluid shear stress.[41] Another study by DePaola et al[42] showed that endothelial Cx43 protein expression increased and decreased with increasing and decreasing blood flow levels. With regard to our data, it would be intriguing to analyze blood flow velocity, wall shear stress, and Cx43 protein expression in CAM vessels before and after short-term and long-term GJ blockade. Further studies are needed to clarify these aspects.

The above-mentioned observations might have different clinical implications. Maldistribution and functional shunting have been identified as pathophysiologic driving forces during shock or ischemia-reperfusion.[43] In this context, it was also shown that bacterial lipopolysaccharides, an initiating factor in sepsis, attenuate cell-to-cell communication, most likely by altering the phosphorylation status of different Cxs.[44,45] With the limitation that the experimental setup provided here cannot mimic the complex conditions leading to sepsis, our data give in vivo evidence that break-down of gap junctional function results in microcirculatory changes similar to those seen in sepsis (malperfusion, hypoxia) and maybe even disseminated intravascular coagulation (stasis/thrombosis).[46]
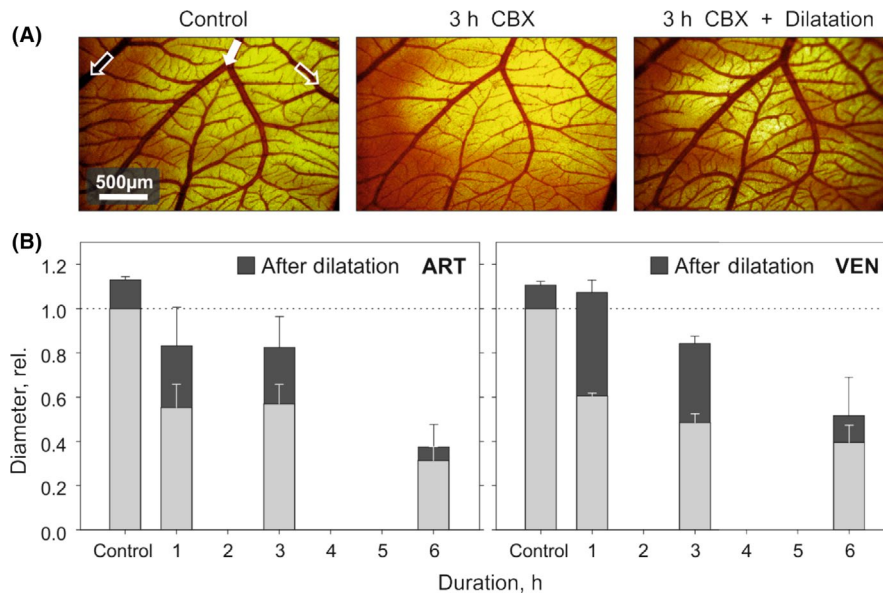
FIGURE 6 Vasodilatation of CAM ART (filled arrows) and VEN (open arrows) before and after treatment with CBX. Vasodilatation was achieved by topical application of 10 μmol/L Ach, 100 μmol/L ADO, 200 μmol/L PAP, and 10 μmol/L SNP for 15 min. A, CAM micrographs before (Control) and after 3 h of treatment with 175 μmol/L CBX. The CBX-treated CAM section was then exposed to the vasodilatory substances (3 h CBX + dilatation). B, Vasodilatation of CAM ART and VEN before (Control) and after incubation with 175 μmol/L CBX. Initially, vasodilatation almost restored resting vessel diameters of CBX-treated vessels. Subsequently, vessel reaction upon dilatation diminished and CBX-induced diameter reduction became structurally dominated. Data are given as means ± SEM for at least N = 92 ART (VEN) in n = 3 CAMs

Tumor microvascular networks are characterized by high structural and functional heterogeneity in which excessively and poorly perfused tissue areas coexist in close neighborhood.[20] Considering in vitro data—VEGF, a proangiogenic factor elevated in most solid tumor, was shown to block endothelial cell-cell communication[47]—and results from mathematical modeling our group hypothesized that impaired GJ-based intercellular communication leading to functional shunting plays a significant role in this process.[48] Although the formation of direct shunt pathways in response to GJ blockade could not be observed in this study, malperfusion might still be related to functional shunting. CAM blood flow could pass by network areas deprived of GJ communication using the remaining pathways mirroring systemic shunting. With regard to tumor tissue, loss of GJ function might cause malperfused and hypoxic tissue areas prone to genetic instability, metastasis[49] and probably even further dysfunction of GJs (eg, hypoxia results in the loss of Cx43 function in the myocardium).[50]

Blood vessels of vascular beds responsible for oxygen uptake (eg, pulmonary or fetoplacental beds like the CAM) constrict in response to hypoxia.[51-54] In this context, we have reported an essential role for Cxs in the mediation of hypoxic pulmonary vasoconstriction.[55] Our present observations suggest that the role of GJs in fetoplacental beds such as the CAM expands beyond mediating vasoconstrictive responses.

Firstly, GJs are responsible for transferring vasodilatory signals from capillaries to arterioles in order to maintain low-resting tone of these vessels (ART 10 ± 1%, VEN 6 ± 4%, Figure 6). This reflects the function of the CAM as a facilitator of maximal gas exchange for a continuously growing embryo. Varying functional demands caused by different states of rest and work that occur in striated muscular tissue, for example, do not exist in the CAM. This removes the need for high-resting tones that allow rapid up- and downregulation of blood flow.[22] By properly adapting vessel tone to the functional demand of the organism, GJs might also play a role in optimizing the energetic cost of vascular networks. De Wit et al pointed out that information transfer via GJs is critical for the matching of oxygen delivery and tissue needs in a well-tuned fashion.[56]

Secondly, GJs play a role in chronic remodeling of CAM vessels. After 6 hours of incubation with CBX, vessel reaction upon vasodilatation declines, suggesting structural remodeling of the vascular bed. This finding is in agreement with studies performed by Bakker and Van Bavel[57,58] who demonstrated that long-term increase of VT is a major driving force in vessel remodeling by structural adaptation. Similarly, acute hypoxia results in vasoconstriction in the lung, while chronic hypoxia causes vascular remodeling and vessel rarefaction.

However, several important aspects of this remodeling process are still unclear. First, the underlying molecular mechanisms that trigger vascular remodeling in the CAM (eg, changes in calcium signaling) remain to be elucidated. Secondly, the CX distribution data suggest that a direct, Cx-mediated change in tone and structure should be restricted to the arteriolar side of CAM vasculature but observed vessel diameter changes are equally strong on the venous side. Based on previous studies on vascular reaction to reduced perfusion including simulation studies of structural vascular adaptation,[18,24] it may be assumed that changes on the venular side reflect

the reduction of blood flow through the CAM network. This concept demands further investigations including histological and modeling approaches.

PERSPECTIVE

In summary, GJs are important for network homeostasis by acutely regulating vessel tone and by chronically regulating vascular structure and vessel remodeling. The molecular mechanisms by which gap junctional communication orchestrates these processes remain to be elucidated. Our data provide novel insight into the complex role of GJs in the regulation and adaptation of vascular networks in vivo and expand our knowledge on systemic vascular adaptation.

DISCLOSURE

The authors declare no conflict of interest.

ORCID

Bianca Nitzsche 🔟 https://orcid.org/0000-0001-7916-3344

REFERENCES

1. Mese G, Richard G, White TW. Gap junctions: basic structure and function. *J Invest Dermatol*. 2007;127(11):2516-2524.
2. Hervé J, Dhein S. Cardiovascular gap junctions. In: Dhein S ed. *Pharmacology of Cardiovascular Gap Junctions*, Vol. 42. Basel: Karger; 2006:107-131.
3. Sohl G, Willecke K. Gap junctions and the connexin protein family. *Cardiovasc Res*. 2004;62:228-232.
4. De Wit C. Connexins pave the way for vascular communication. *News Physiol Sci*. 2004;19:148-153.
5. Simon AM, McWhorter AR. Vascular Abnormalities in mice lacking the endothelial gap junction proteins connexin37 and connexin40. *Dev Biol*. 2002;251(2):206-220.
6. Simon AM, McWhorter AR. Role of connexin37 and connexin40 in vascular development. *Cell Commun Adhes*. 2003;10:379-385.
7. Gartner C, Ziegelhoffer B, Kostelka M, Stepan H, Mohr FW, Dhein S. Knock-down of endothelial connexins impairs angiogenesis. *Pharmacol Res*. 2012;65(3):347-357.
8. Liao Y, Day KH, Damon DN, Duling BR. Endothelial cell-specific knockout of connexin 43 causes hypotension and bradycardia in mice. *Proc Natl Acad Sci USA*. 2001;98(17):9989-9994.
9. Segal SS, Duling BR. Flow control among microvessels coordinated by intercellular conduction. *Science*. 1986;234(4778):868-870.
10. de Wit C, Wolfle SE. EDHF and gap junctions: important regulators of vascular tone within the microcirculation. *Curr Pharm Biotechnol*. 2007;8(1):11-25.
11. Rivers RJ. Cumulative conducted vasodilation within a single arteriole and the maximum conducted response. *Am J Physiol*. 1997;273(1 Pt 2):H310-H316.
12. de Wit C, Roos F, Bolz S-S, et al. Impaired conduction of vasodilation along arterioles in connexin40-deficient mice. *Circ Res*. 2000;86(6):649-655.
13. de Wit C. Different pathways with distinct properties conduct dilations in the microcirculation in vivo. *Cardiovasc Res*. 2010;85:604-613.
14. Hoepfl B, Rodenwaldt B, Pohl U, De Wit C. EDHF, but not NO or prostaglandins, is critical to evoke a conducted dilation upon ACh in hamster arterioles. *Am J Physiol Heart Circ Physiol*. 2002;283(3):H996-H1004.
15. Siegl D, Koeppen M, Wolfle SE, Pohl U, de Wit C. Myoendothelial coupling is not prominent in arterioles within the mouse cremaster microcirculation in vivo. *Circ Res*. 2005;97(8):781-788.
16. Kurjiaka DT, Segal SS. Conducted vasodilation elevates flow in arteriole networks of hamster striated muscle. *Am J Physiol*. 1995;269(5 Pt 2):H1723-H1728.
17. Pries AR, Secomb TW, Gaehtgens P. Structural adaptation and stability of microvascular networks: theory and simulations. *Am J Physiol*. 1998;275(2 Pt 2):H349-360.
18. Pries AR, Reglin B, Secomb TW. Structural adaptation of microvascular networks: functional roles of adaptive responses. *Am J Physiol Heart Circ Physiol*. 2001;281(3):H1015-H1025.
19. Pries AR, Reglin B, Secomb TW. Structural response of microcirculatory networks to changes in demand: information transfer by shear stress. *Am J Physiol Heart Circ Physiol*. 2003;284:H2204-H2212.
20. Pries AR, Cornelissen A, Sloot AA, et al. Structural adaptation and heterogeneity of normal and tumor microvascular networks. *PLoS Comput Biol*. 2009;5(5):e1000394.
21. Secomb TW, Alberding JP, Hsu R, Dewhirst MW, Pries AR. Angiogenesis: an adaptive dynamic biological patterning problem. *PLoS Comput Biol*. 2013;9(3):e1002983.
22. Maibier M, Reglin B, Nitzsche B, et al. Structure and hemodynamics of vascular networks in the chorioallantoic membrane of the chicken. *Am J Physiol Heart Circ Physiol*. 2016;311(4):H913-H926.
23. Rasband WS. ImageJ. U.S. National Institutes of Health, Bethesda, Maryland, USA; 1997–2005. http://rsb.info.nih.gov/ij/
24. Xiang W, Reglin B, Nitzsche B, et al. Dynamic remodeling of arteriolar collaterals after acute occlusion in chick chorioallantoic membrane. *Microcirculation*. 2017;24(4):e12351.
25. Schrotter S, Leondaritis G, Eickholt BJ. Capillary isoelectric focusing of Akt isoforms identifies highly dynamic phosphorylation in neuronal cells and brain tissue. *J Biol Chem*. 2016;291(19):10239-10251.
26. Wright CS, van Steensel MA, Hodgins MB, Martin PE. Connexin mimetic peptides improve cell migration rates of human epidermal keratinocytes and dermal fibroblasts in vitro. *Wound Repair Regen*. 2009;17(2):240-249.
27. Nitzsche B, Gloesenkamp C, Schrader M, et al. Novel compounds with antiangiogenic and antiproliferative potency for growth control of testicular germ cell tumours. *Br J Cancer*. 2010;103(1):18-28.
28. Tang E, Vanhoutte PM. Gap junction inhibitors reduce endothelium-dependent contractions in the aorta of spontaneously. *Hypertensive Rats*. 2008;327(1):148-153.
29. Edwards G, Feletou M, Gardener MJ, Thollon C, Vanhoutte PM, Weston AH. Role of gap junctions in the responses to EDHF in rat and guinea-pig small arteries. *Br J Pharmacol*. 1999;128(8):1788-1794.
30. Tare M, Coleman HA, Parkington HC. Glycyrrhetinic derivatives inhibit hyperpolarization in endothelial cells of guinea pig and rat arteries. *Am J Physiol Heart Circ Physiol*. 2002;282(1):H335-H341.
31. Dhein S, Hammerath SB. Aspects of the intercellular communication in aged hearts: effects of the gap junction uncoupler palmitoleic acid. *Naunyn Schmiedebergs Arch Pharmacol*. 2001;364(5):397-408.
32. Domenighetti AA, Beny JL, Chabaud F, Frieden M. An intercellular regenerative calcium wave in porcine coronary artery endothelial cells in primary culture. *J Physiol*. 1998;513(Pt 1):103-116.
33. Dhein S, Krusemann K, Schaefer T. Effects of the gap junction uncoupler palmitoleic acid on the activation and repolarization wavefronts in isolated rabbit hearts. *Br J Pharmacol*. 1999;128(7):1375-1384.
34. Chaytor AT, Martin PE, Edwards DH, Griffith TM. Gap junctional communication underpins EDHF-type relaxations evoked by ACh in the rat hepatic artery. *Am J Physiol Heart Circ Physiol*. 2001;280(6):H2441-H2450.

35. Begandt D, Bader A, Dreyer L, Eisert N, Reeck T, Ngezahayo A. Biphasic increase of gap junction coupling induced by dipyridamole in the rat aortic A-10 vascular smooth muscle cell line. *J Cell Commun Signal.* 2013;7:151-160.

36. Radtke J, Schmidt K, Wulff H, Kohler R, de Wit C. Activation of KCa3.1 by SKA-31 induces arteriolar dilatation and lowers blood pressure in normo- and hypertensive connexin40-deficient mice. *Br J Pharmacol.* 2013;170(2):293-303.

37. Feletou M. Endothelium-dependent hyperpolarization and endothelial dysfunction. *J Cardiovasc Pharmacol.* 2016;67(5):373-387.

38. Leybaert L, Lampe PD, Dhein S, et al. Connexins in cardiovascular and neurovascular health and disease: pharmacological implications. *Pharmacol Rev.* 2017;69(4):396-478.

39. Michel T, Vanhoutte PM. Cellular signaling and NO production. *Pflugers Arch.* 2010;459(6):807-816.

40. Busse R, Edwards G, Feletou M, Fleming I, Vanhoutte PM, Weston AH. EDHF: bringing the concepts together. *Trends Pharmacol Sci.* 2002;23(8):374-380.

41. Cowan DB, Lye SJ, Langille BL. Regulation of vascular connexin43 gene expression by mechanical loads. *Circ Res.* 1998;82(7):786-793.

42. DePaola N, Davies PF, Pritchard WF Jr, Florez L, Harbeck N, Polacek DC. Spatial and temporal regulation of gap junction connexin43 in vascular endothelial cells exposed to controlled disturbed flows in vitro. *Proc Natl Acad Sci USA.* 1999;96(6):3154-3159.

43. Lauterbach M, Horstick G, Plum N, Weilemann LS, Munzel T, Kempski O. Shunting of the microcirculation after mesenteric ischemia and reperfusion is a function of ischemia time and increases mortality. *Microcirculation.* 2006;13(5):411-422.

44. Tyml K. Role of connexins in microvascular dysfunction during inflammation. *Can J Physiol Pharmacol.* 2011;89(1):1-12.

45. Lidington D, Ouellette Y, Tyml K. Endotoxin increases intercellular resistance in microvascular endothelial cells by a tyrosine kinase pathway. *J Cell Physiol.* 2000;185(1):117-125.

46. Iba T, Watanabe E, Umemura Y, et al. Sepsis-associated disseminated intravascular coagulation and its differential diagnoses. *J Intensive Care.* 2019;7:32.

47. Suarez S, Ballmer-Hofer K. VEGF transiently disrupts gap junctional communication in endothelial cells. *J Cell Sci.* 2001;114(Pt 6):1229-1235.

48. Pries AR, Hopfner M, le Noble F, Dewhirst MW, Secomb TW. The shunt problem: control of functional shunting in normal and tumour vasculature. *Nat Rev Cancer.* 2010;10(8):587-593.

49. Bottaro DP, Liotta LA. Out of air is not out of action. *Nature.* 2019;423(6940):593.

50. Solan JL, Marquez-Rosado L, Sorgen PL, Thornton PJ, Gafken PR, Lampe PD. Phosphorylation at S365 is a gatekeeper event that changes the structure of Cx43 and prevents down-regulation by PKC. *J Cell Biol.* 2007;179:1301-1309.

51. Hampl V, Jakoubek V. Regulation of fetoplacental vascular bed by hypoxia. *Physiol Res.* 2009;58(Suppl 2):S87-S93.

52. Hampl V, Bíbová J, Straňák Z, et al. Hypoxic fetoplacental vasoconstriction in humans is mediated by potassium channel inhibition. *Am J Physiol Heart Circ Physiol.* 2002;283(6):H2440-H2449.

53. Lindgren I, Zoer B, Altimiras J, Villamor E. Reactivity of chicken chorioallantoic arteries, avian homologue of human fetoplacental arteries. *J Physiol Pharmacol.* 2010;61(5):619-628.

54. Sommer N, Strielkov I, Pak O, Weissmann N. Oxygen sensing and signal transduction in hypoxic pulmonary vasoconstriction. *Eur Respir J.* 2016;47(1):288-303.

55. Wang L, Yin J, Nickles HT, et al. Hypoxic pulmonary vasoconstriction requires connexin 40-mediated endothelial signal conduction. *J Clin Invest.* 2012;122(11):4218-4230.

56. Schmidt VJ, Wolfle SE, Boettcher M, de Wit C. Gap junctions synchronize vascular tone within the microcirculation. *Pharmacol Rep.* 2008;60(1):68-74.

57. Bakker EN, van der Meulen ET, van den Berg BM, Everts V, Spaan JA, VanBavel E. Inward remodeling follows chronic vasoconstriction in isolated resistance arteries. *J Vasc Res.* 2002;39(1):12-20.

58. Van Bavel E, Bakker EN, Pistea A, Sorop O, Spaan JA. Mechanics of microvascular remodeling. *Clin Hemorheol Microcirc.* 2006;34(1-2):35-41.